

Statistics of Si-O bond-breakage rate variations induced by O-Si-O angle fluctuations

S.E. Tyaginov*, V. Sverdlov, W. Göös*, T. Grasser*

(*)Christian Doppler Laboratory for TCAD at the Institute for Microelectronics

TU Wien, Gußhausstraße 27-29

Vienna A-1040, Austria

{tyaginov|sverdlov|goes|grasser}@iue.tuwien.ac.at

Abstract— The McPherson model for the Si-O bond-breakage has been extended in a manner to capture the effect of O-Si-O angle variations on the breakage rate. Using a distribution function of the O-Si-O bond angle, a series of breakage rate probability densities has been calculated as a function of the applied electric field. Using such a distribution function we have calculated the mean value and the standard deviation of the breakage rate and compare them to the nominal rate corresponding to the fixed angle of 109.48° observed in crystalline α -quartz. It is shown that the mean value of this rate is substantially higher than and the standard deviation is comparable with the nominal rate. Obtained dependencies demonstrate a linear trend in a log-lin space, thereby validating the thermo-chemical model for the time-dependent-dielectric breakdown also in the case of non-uniform O-Si-O angle distribution typical for amorphous silica.

Keywords—silicon-oxygen bond, bond-breakage rate, bond angle fluctuations, amorphous silica, WKB approximation, tunneling

I. INTRODUCTION

In contrast to crystalline α -quartz, amorphous SiO_2 is characterized by a wide spread of O-Si-O and Si-O-Si angles. A lot of either experimental or theoretical [1-5] data regarding bond angle fluctuations has been reported in the literature demonstrating rather broad distributions. These variations affect the electronic structure of the material [6], hole trapping energetics [7], and act as precursors for structural disorder [8]. It is obvious that the presence of substantial angle dispersion leads to a strong weakening of the Si-O bond, thereby abruptly decreasing the breakage probability.

Since silicon-oxygen bond rupture has been suspected to be an important contributor to hot-carrier-injection related damage [9] and to time-dependent-dielectric breakdown [10], we expect bond weakening induced by O-Si-O/Si-O-Si angle variations to be a very important issue in the field of the reliability of SiO_2 gate layers. In spite of the success of the Si-O bond-breakage model proposed by McPherson [10], the effect of bond angle variations on the Si-O energetics has not been rigorously analyzed so far, and only speculations concerning its importance have been given.

Therefore, the purpose of this work is to extend the McPherson model by considering the impact of bond angle fluctuations on the Si-O bond-breakage energetics.

II. SI-O BOND-BREAKAGE: GENERAL CONSIDERATIONS

Similar to the original model, the breakage of the Si-O bond is considered as a transition of the Si ion from the 4-fold coordination in the center of the SiO_4 tetrahedron to the 3-fold position beyond the O_3 plane (Fig. 1, inset) followed by the formation of a Si-Si bridge. This transition is considered as a superposition of a thermionic excitation over the potential barrier and quantum mechanical tunneling from the primary to the secondary minimum. Such a profile represents the dependence of the binding potential on the Si ion displacement from its equilibrium position in the center of the SiO_4 tetrahedron perpendicular to the O_3 plane. The potential is calculated considering 4 contributions related to interactions of the silicon ion with four surrounding oxygen ones.

These Si-O interactions have been treated by using the Mie-Grüneisen pair-wise interatomic potential:

$$\Phi(r) = \Phi_B \left[A^{(9)}(r/r_0)^9 + A^{(2)}(r/r_0)^2 + A^{(1)}(r/r_0) \right], \quad (1)$$

where Φ_B and r_0 denote the bond strength and length, while constants $A^{(9)}$, $A^{(2)}$, $A^{(1)}$ are determined in order to represent the energetical and spatial positions of the equilibrium configuration as well as the bond polarity [10].

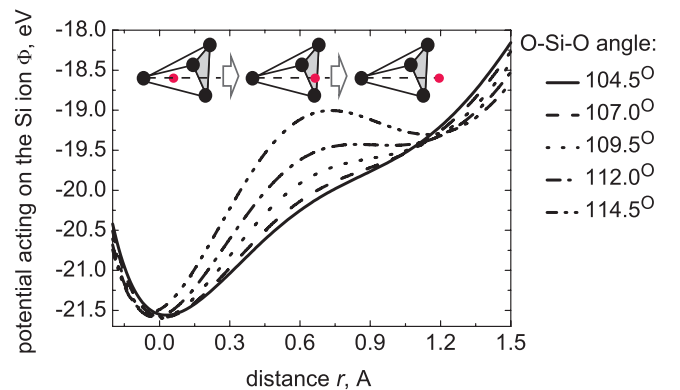


Figure 1. Transformations of the barrier profile due to O-Si-O angle variations. Inset: Si ion transition through and beyond the O_3 plane.

Tunneling of the Si ion is treated within the WKB approximation. Energetical positions of eigenstates E_n (with n as the quantum number) in the quantum well of the primary

minimum, tunnel probabilities from each level T_n and the attempt frequency (the reciprocal aller-retour time) $1/\tau_{n,a-r}$ are determined using these expressions [10,11]:

$$\int_{x_1}^{x_2} \sqrt{2m_{Si}(E_n - V(x))} dx = (n+1/2)\pi\hbar \quad (2a)$$

$$T_n = \exp\left(-\frac{2}{\hbar} \int_{x_2}^{x_3} \sqrt{2m_{Si}[V(x) - E_n]} dx\right) \quad (2b)$$

$$\tau_{a-r,n} = 2\sqrt{\frac{m_{Si}}{2}} \int_{x_1}^{x_2} \frac{dx}{\sqrt{E_n - V(x)}}, \quad (2c)$$

with $V(x)$ being the potential profile, m_{Si} is the Si ion mass, while $[x_1; x_2]$ and $[x_2; x_3]$ denote intervals of classically allowed and prohibited ion movement.

The portion of the ‘‘tunnel flux of Si ions’’ from the n -th level is written as the product of the quantity of available particles f_n , the tunnel probability T_n , and the attempt frequency $1/\tau_{n,a-r}$, i.e.

$$P_{tu,n} = \frac{f_n T_n}{\tau_{a-r,n}}. \quad (2d)$$

The level occupation f_n is obtained with the Boltzmann distribution:

$$f_n = \exp(-E_n/k_B T) / \sum_n \exp(-E_n/k_B T), \quad (2e)$$

where k_B and T are the Boltzmann constant and the absolute temperature, while the statistical sum in the denominator over all levels ensures the probability normalization.

The thermionic excitation of the Si ion over the potential barrier is characterized with the corresponding rate:

$$P_{th} = \nu \cdot \exp(-E_a/kT), \quad (2f)$$

where $\nu \sim 10^{12} \dots 10^{13} \text{ s}^{-1}$ is the attempt frequency and E_a is the activation energy (barrier height).

Summing the rates $P_{tu,n}$ over all energy levels one obtains the total tunnel rate P_{tu} , while the total bond-breakage rate (calculated taking into account both tunneling and thermionic mechanisms) is to be found as:

$$P = P_{tu} + P_{th}. \quad (2h)$$

III. Si-O BOND-BREAKAGE: EFFECT OF ANGLE VARIATIONS

Fig. 1 shows the transformation of the potential profile induced by O-Si-O angle φ (Fig.2, inset) variations. The secondary minimum becomes deeper while φ grows and simultaneously the bond-breakage activation energy increases. For a fixed value of φ typical for α -quartz ($\varphi_n = 109.48^\circ$) the secondary minimum position is determined by the equilateral O_3 triangle and thus related to the direction of the SiO_4 tetrahedron symmetry axis. While calculating the binding potential as a function of the Si ion displacement in the

McPherson direction (Fig.1, inset), three oxygen ions in the O_3 plane provide equal contributions to the energy and therefore with an O ion being shifted (due to angle φ variations) from its position in a vortex of the regular SiO_4 tetrahedron the symmetry is lost(???) and the secondary energy minimum is found in another direction.

Since Si ‘‘finds’’ a direction characterized by the highest bond-breakage rate P (highest probability for a transition perpendicular and beyond the O_3 plane) and will break the SiO_4 tetrahedral configuration just in this way, one needs to find the direction – defined by the angle θ , (see inset of Fig. 2) – for which the maximal P (referred hereafter as bond-breakage rate) is obtained. For this purpose we used the multidimensional downhill simplex method [12]. This maximization was done in a two-dimensional space, i.e. directions in which the maximal P is to be found are parameterized by 2 coordinates in the O_3 plane. For $\varphi_n = 109.48^\circ$, the spatial position of the secondary minimum corresponds to the direction at which the maximal P is obtained, i.e. $\theta = 0$ (a case of a regular SiO_4 tetrahedron, i.e. $\varphi_n = 109.48^\circ$ which is typical for α -quartz). While performing the maximization procedure we considered only those directions that demonstrated a pronounced secondary minimum.

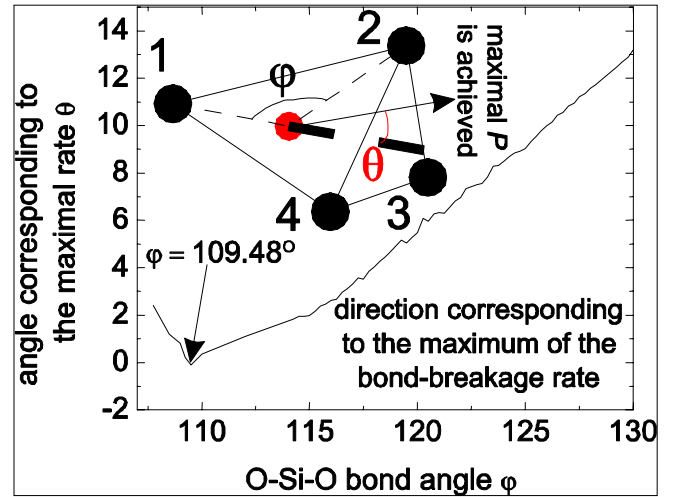


Figure 2. The dependence of angle θ on O-Si-O angle. Inset: angle θ between the direction of the maximal P and the SiO_4 symmetry axis

The dependence of θ on φ is plotted in Fig. 2. The secondary minimum appears at the angle $\varphi_{cr} \approx 107.75^\circ$. Since its appearance is due to the contribution of the 3 O ions, for $\varphi < 109.48^\circ$ a direction corresponding to the maximal P is rotated toward the deviated O ion (marked as No. 2 in Fig. 2, inset). For $\varphi \approx 109.48^\circ$ this direction coincides with the symmetry axis of the tetrahedron ($\theta = 0$). For higher φ the maximal P is found at the opposite side relative to the symmetry axis.

Fig. 3 demonstrates the dependence of the bond-breakage rate P on the angle φ calculated for several values of the applied field. The abrupt increase of P which is seen in Fig. 3 for all fields F corresponds to the appearance of a secondary

minimum at $\varphi = \varphi_{cr}$. Fig. 3 shows that curves calculated for different F are equidistantly spaced. Such a behavior means that each (fixed) step in F increases the rate P by the same factor and reveals the same activation bond-breakage nature typical for a wide range of bond angles φ .

Fig. 4 depicts a series of curves $P = P(F)$ calculated for various parameters φ and explicitly demonstrates an exponential dependence of the bond-breakage rate vs. the electric field. This circumstance supports the thermo-chemical model treating the breakage of the Si-O bond in terms of a chemical reaction characterized with a certain activation energy. Within this model this activation energy is being reduced proportionally to the increasing electric field and the linear interrelation between the logarithmic time-to-failure (which is related to the probability of bond rupture) and the field F is thus obtained.

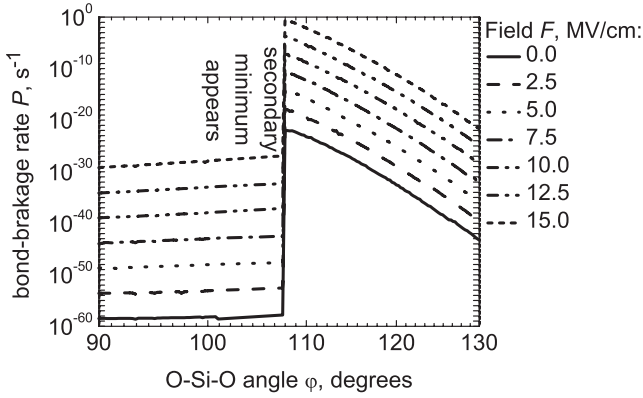


Figure 3. The bond-breakage rate vs. O-Si-O angle for various fields F .

IV. STATISTICS OF THE BOND-BREAKAGE RATE

In order to calculate the parameters of the statistical variation of P we used the probability density $D_\varphi(\varphi)$ of the variate φ borrowed from [1] (Fig. 5, left inset). To evaluate the distribution function $D_P(P)$ for the variate P we truncated the dependence $P(\varphi)$ at φ_{cr} since the values corresponding to smaller angles are not informative and therefore obtained a single-valued reciprocal dependency $\varphi(P)$.

The probability density $D_P(P)$, the mean value $\langle P \rangle$ and the standard deviation σ_P of the rate P are found as:

$$D_P(P, F) = D_\varphi(\varphi(P, F)) \left| \frac{d\varphi(P, F)}{dP} \right| \quad (3a)$$

$$\langle P \rangle (F) = \int P(\varphi, F) D_\varphi(\varphi) d\varphi \quad (3b)$$

$$\sigma_P(F) = \left(\int (P(F) - \langle P \rangle (F))^2 D_\varphi(\varphi) d\varphi \right)^{1/2} \quad (3c)$$

The probability densities for various F are shown in Fig. 5. Since $D_\varphi(\varphi)$ has a maximum at $\varphi \approx 109.48^\circ$ and decays while moving away from this value, $D_P(P)$ should also reveal a maximum shifted due to the contribution of $|d\varphi/dP|$ which

reduces with the variate P . In fact, in the range of varying angle φ from $\varphi_{cr} \approx 107.75^\circ$ to $\varphi_n = 109.84^\circ$, the component $D_\varphi(\varphi)$ grows with φ while $|d\varphi/dP|$ rapidly decreases and thus the minimum at $D_P(P)$ is expected to be shifted from $\varphi = \varphi_n$ toward smaller angles. However, $|d\varphi/dP|$ decays much faster than $D_\varphi(\varphi)$ and thereby only a hint on a maximum (Fig. 5, right inset) is visible.

The mean value $\langle P \rangle$ and the standard deviation σ_P vs. F are plotted in Fig. 6. The nominal bond-breakage rate P_n calculated for the fixed angle $\varphi_n \approx 109.48^\circ$ is also shown in Fig. 6 as a reference. Note that all the curves have the same linear behavior in a log-lin scale.

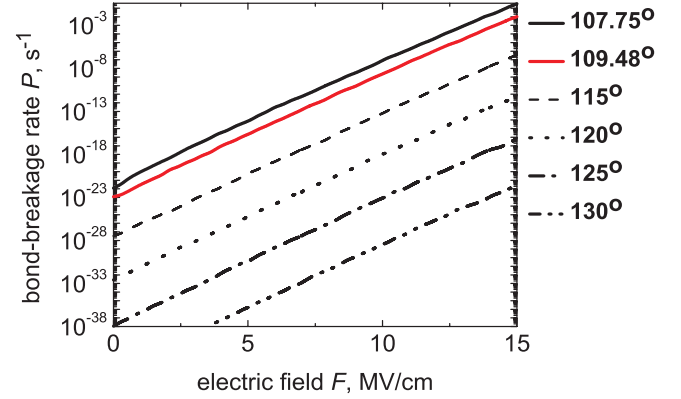


Figure 4. The breakage rate vs. field plotted for various O-Si-O angles.

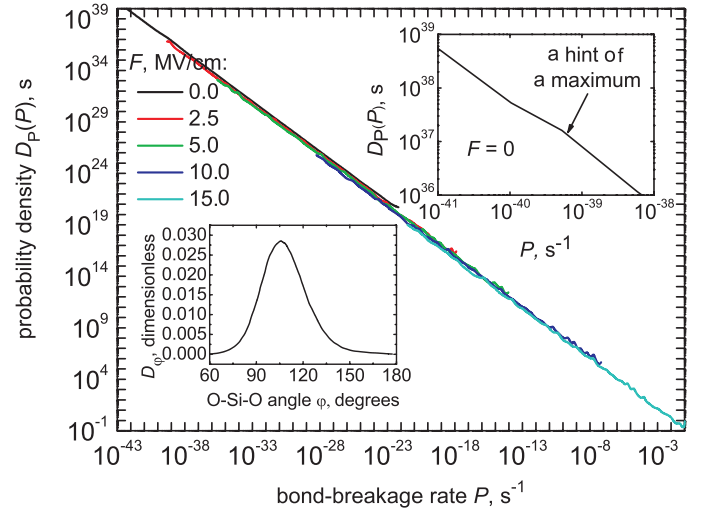


Figure 5. The distribution functions of P calculated for various F . Left inset: the probability density of φ ; right: a hint of a maximum at the curve $D_P(P)$ for $F = 0$.

A property of the $D_P(P)$ is that the field F does not change the form of the curves, shifting them as a whole towards higher P . This is related to the equidistance of the curves $P(\varphi)$ plotted with a fixed step on F . Another consequence of this equidistance is a similar log-lin slope of all curves: $\langle P \rangle (F)$, $\sigma_P(F)$ and $P_n(F)$ (Fig. 6, left inset). This behavior supports the thermo-chemical model [10] even in the case of strongly fluctuating O-Si-O angles, when the mean value of the bond-

breakage rate $\langle P \rangle$ rather than P_n should be considered. In a wide range of electric field F , the mean bond-breakage rate $\langle P \rangle$ is more than 5 times larger than the nominal one, P_n and the deviation σ_p is comparable to P_n .

While a percolation path throughout the oxide film is being created during the electrical stress, pre-existing defects act as precursors for the formation of clusters eventually uniting into one, connecting the opposite interfaces of the film, i.e. to a percolation path. In fact, as it was reported in [13], if a defect already exists, another will be generated predominately in the vicinity of the first one. Thus a large span of P (reflected by a large standard deviation σ_d) complicates the matter, because existence of huge values of P (even realized with a small probability) are linked to the precursors for defect creation.

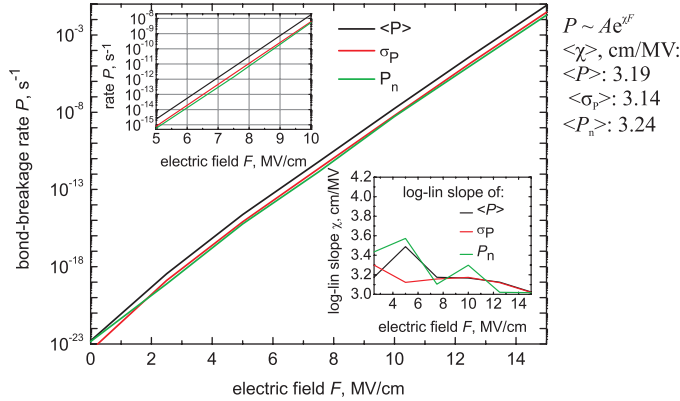


Figure 6. Mean rate $\langle P \rangle$, deviation σ_p and nominal rate P_n vs. F . Left inset: a fragment of the main plot; right inset: the slope of the curves

V. CONCLUSION

Based on the original McPherson model for the silicon-oxygen rupture, which uses a fixed O-Si-O angle φ , we suggest a modification to also capture the impact of angle φ fluctuations on the Si-O bond-breakage rate.

It is shown that the secondary energetical minimum required for the bond rupture exists only for $\varphi > \varphi_{cr} = 107.75^\circ$. We calculated the angle θ between the SiO_4 tetrahedron symmetry axis and the direction in which the saddle point is revealed as a function of φ demonstrating a zero angle θ for $\varphi = 109.48^\circ$ (the case of the original McPherson model). Such a dependence has been used for evaluation of the distribution function $D_p(P)$ of the variate P .

Also a set of dependencies $P = P(\varphi)$ for several values of applied electric fields has been calculated demonstrating an abrupt increase of the breakage rate at $\varphi = 107.75^\circ$ (the angle of occurrence of the secondary minimum). Note that curves obtained for different F (varying with a fixed step) are spaced equidistantly on a log-lin scale, while $P = P(F)$ shows an exponential behavior.

A linear shape (on a log-lin scale) of the distribution $D_p(P)$ for the variate P (the probability density of P does not change the shape with F and is just being shifted parallel) combined with the linear relation between $\ln P$ and F leads to an exponential dependence of the nominal P_n , the mean value $\langle P \rangle$, and the standard deviation σ_p of the breakage rate on the electric field. Such a behavior results in the same slope of $\langle P \rangle(F)$, $\sigma_p(F)$ and $P_n(F)$ and suggests that also in a case of fluctuating φ the electro-chemical model provides a good prediction for time-to-breakdown vs. F .

Note that the mean value $\langle P \rangle$ is more than 5 times larger than the nominal rate P_n while its standard deviation σ_p is comparable to P_n assuming a quite wide span of the variate P . Such a large span of P complicates the picture, because existence of huge values of P (realized with a small probability) serve as precursors for defect creation.

REFERENCES

- [1] A. Carré, J. Horbach, S. Ispas, W. Kob, "New fitting scheme to obtain effective potential from Car-Parrinello molecular-dynamics simulations: Application to silica", *Lett. Journ. Expl. Front. Phys.*, Vol. 82, pp. 17001-17010. 2008.
- [2] S.V. Alifhan, A. Kuronen, K. Kaski, "Realistic models for amorphous silica: a comparative study of different potentials", *Phys. Rev. B*, v. 68, pp. 073203-1 (2003).
- [3] S. Munetoh, T. Motooka, K. Morihuchi, A. Shintani, "Interatomic potential for Si-O systems using Tersoff parameterization", *Comput. Mater. Sci.*, v. 39, pp. 334-339 (2007).
- [4] M.G. Tucker, D.A. Keen, M.T. Dove, K. Trachenko, "Refinement of the Si-O-Si bond angle distribution in vitreous silica", *J. Phys.: Condens. Matter*, v.17, pp. S67-S75 (2005).
- [5] C.R. Helms, E.H. Poindexter, "The silicon-silicon-dioxide system: its microstructure and imperfections", *Rep. Prog. Phys.*, v. 57, pp. 791-852 (1994).
- [6] R. N. Nucho, A. Madhukar, "Electronic structure of SiO_2 : α -quartz and the influence of local disorder", *Phys. Rev. B*, Vol. 21. pp. 1576-1588 (1980).
- [7] X. Zhang, C.K. Ong, "Hole trapping properties of germanium in alpha - quartz", *J. Phys.: Condens. Matter*, Vol., pp. 1603-1615 1995.
- [8] P.E.M. Lopes, E. Demchuk, A.D. Mackerell, "Reconstruction of the (011) surface on alpha-quartz: a semiclassical *ab initio* molecular dynamics study" *Int. Journ. Quant. Chem.*, v. 109, pp. 50-64, 2009.
- [9] D. Saha, D. Varghese, S. Mahapatra, "Role of anode hole injection and valence band hole tunneling on interface trap generation during hot carrier injection stress", *IEEE Electron Dev. Lett.*, v. EDL-27, pp. 585-587, 2006.
- [10] J.W. McPherson, "Quantum mechanical treatment of Si-O bond breakage in silica under time dependent dielectric breakdown", *Proceedings of IRPS-2007*, pp. 209-215, 2007
- [11] M.I. Vexler, "A simple quantum model for the MOS structure in accumulation mode", *Solid-State Electron.*, v. 47. pp. 1283-1287 (2003).
- [12] W.H. Press, A.A. Teukolsky, W.T. Vetterling, B.P. Flannery, "Numerical Recipes in C", Cambridge University Press, 1997.
- [13] G. Bersuker, A. Korin, L. Fonseca, A. Safonov, A. Bagatur'yants, H.R. Ruff, "The role of localized states in the degradation of thin gate oxides", *Microel. Engin.*, v. 69, pp. 118-129, 2003.